PHILOSOPHICAL TRANSACTIONS OF THE ROYAL SOCIETY A MATHEMATICAL, PHYSICAL & ENGINEERING SCIENCES

The effect of particle size, shape, distribution and their evolution on the constitutive response of nonlinearly viscous composites. II. Examples

M. Kailasam, P. Ponte Castañeda and J. R. Willis

Phil. Trans. R. Soc. Lond. A 1997 **355**, 1853-1872
doi: 10.1098/rsta.1997.0093

The effect of particle size, shape, distribution and their evolution on the constitutive response of nonlinearly viscous composites. II. Examples

By M. Kailasam[1], P. Ponte Castañeda[1] and J. R. Willis[2]

[1]*Department of Mechanical Engineering and Applied Mechanics, University of Pennsylvania, Philadelphia, PA 19104, USA*

[2]*Department of Applied Mathematics and Theoretical Physics, University of Cambridge, Cambridge CB3 9EW, UK*

Part I of this work was concerned with the development of constitutive models for nonlinearly viscous and perfectly plastic composites, which are capable of accounting for the evolution of microstructure when the composites are subjected to finite deformation. This involved the derivation of instantaneous constitutive relations for the composites depending on appropriate microstructural variables, as well as of evolution equations for these variables. As an application of the general theory, in this part of the work, use is made of the models to analyse the response of porous materials and of two-phase composites with perfectly plastic phases under axisymmetric loading conditions (with fixed axes). Attention is focused on the effect of the evolution of the distribution of the inclusions (or voids) on the overall response of the composites. It is found that for porous materials, or for more general classes of composites where the inclusions are softer than the matrix, the effect of changes in the distribution of the inclusions is not very significant relative to the effect of changes in the size and shape of the inclusions. On the other hand, for composites with inclusions that are sufficiently harder than the matrix, the deformation is concentrated in the matrix, and the effect of changes in the distribution function of the inclusions can become quite significant.

1. Introduction

Part I of this work (Kailasam *et al.* 1997) was concerned with the development of constitutive models for two-phase nonlinearly viscous and perfectly plastic composites with evolving microstructures. This involved generalizing the earlier models of Ponte Castañeda & Zaidman (1994) (see also Zaidman & Ponte Castañeda 1996)—which included the effects of the evolution of the shape and size of the voids (inclusions) on the overall response of the composites—to incorporate the ability to account for the effect of the evolution of the spatial distribution of voids (inclusions) on the overall response of the composites, when they are subjected to finite deformation. Henceforth, the above two papers will be referred to as PCZ and ZPC, respectively, for convenience. The constitutive models are formulated in terms of instantaneous effective potentials and yield functions for nonlinearly viscous and perfectly plastic composites, respectively, which depend on appropriate microstructural variables, along with the evolution equations for these variables. The potentials and yield functions were

Phil. Trans. R. Soc. Lond. A (1997) **355**, 1853–1872
Printed in Great Britain

obtained in part I from the recent Hashin–Shtrikman estimates of Ponte Castañeda & Willis (1995) for linear composites with ellipsoidal particulate microstructures via the variational procedure of Ponte Castañeda (1991). For triaxial loading conditions (with fixed loading axes), the following internal variables were selected to characterize the state of the microstructure: the volume fraction and aspect ratios of the inclusions, as well as the aspect ratios of the distribution function of the inclusion centres. Evolution equations for these variables were then developed, which when solved in combination with the instantaneous constitutive equations provide the complete constitutive description of the composite.

In this paper, we shall apply the model developed in part I to porous composites with a perfectly plastic matrix and to two-phase incompressible composites with perfectly plastic phases. It is emphasized that the model can be used for composites with more general nonlinear phases and that perfectly plastic phases have been chosen for the sake of simplicity. We shall consider composites whose microstructure initially consists of an isotropic distribution of spherical inclusions (voids) and are subjected to axisymmetric loadings. We note that the model, in its present form, can be used for composites subjected to general triaxial loading conditions and that axisymmetric loads have been considered only for illustrative purposes. The outline of the paper is as follows. First, in § 2, the case of porous materials is considered and then, in § 3, two-phase composites are studied. Finally, in § 4, some concluding remarks are offered. In each case, yield surfaces for the composites are computed and the influence of the relevant microstructural variables on the yield surfaces is considered. Then, the instantaneous constitutive equations for the composites, which are obtained from the yield functions, are solved in combination with the evolution equations for the appropriate microstructural variables in order to obtain the effective response of the composite when it is subjected to axisymmetric loading. In particular, we focus our attention on the effect of the evolution of the distribution of the inclusions (voids) on the overall response of the composite.

2. Application to porous composites with a perfectly plastic matrix

(*a*) *Effective yield surfaces*

In this section, we obtain estimates for the effective yield surfaces of porous materials. We will consider materials with microstructures that initially consist of isotropic distributions of spherical voids. When such composites are subjected to axisymmetric loads, where the only non-zero components of the stress are $\bar{\sigma}_{11} = \bar{\sigma}_{22}$ and $\bar{\sigma}_{33}$, the microstructure evolves so that the composites exhibit transverse isotropy. The relevant microstructural variables are then the porosity (f), the aspect ratio of the voids (w^{i}) and the aspect ratio of the distribution (w^{d}). It is noted that the effective yield surfaces can be characterized in terms of the non-zero transversely isotropic invariants of the stress, $\bar{\sigma}_p = \frac{1}{2}(\bar{\sigma}_{11} + \bar{\sigma}_{22})$ and $\bar{\sigma}_n = \bar{\sigma}_{33}$. In this case, the effective yield functions are given by expressions of the type (see part I)

$$\tilde{\Phi}(\bar{\boldsymbol{\sigma}}) = \frac{\bar{\boldsymbol{\sigma}} \cdot (\tilde{\boldsymbol{m}}\bar{\boldsymbol{\sigma}})}{1-f} - (\sigma_y^{(1)})^2, \tag{2.1}$$

where $\bar{\boldsymbol{\sigma}} \cdot (\tilde{\boldsymbol{m}}\bar{\boldsymbol{\sigma}})$ is given by expression (5.6) of part I, with $\tilde{\boldsymbol{m}}$ being a function of the microstructural variables, i.e. $\tilde{\boldsymbol{m}} = \tilde{\boldsymbol{m}}(f, w^{\mathrm{i}}, w^{\mathrm{d}})$, and where $(\sigma_y^{(1)})$ denotes the yield stress of the matrix phase. In this section, we study the effect of the aspect ratios of the voids and of their distribution on the effective yield surfaces.

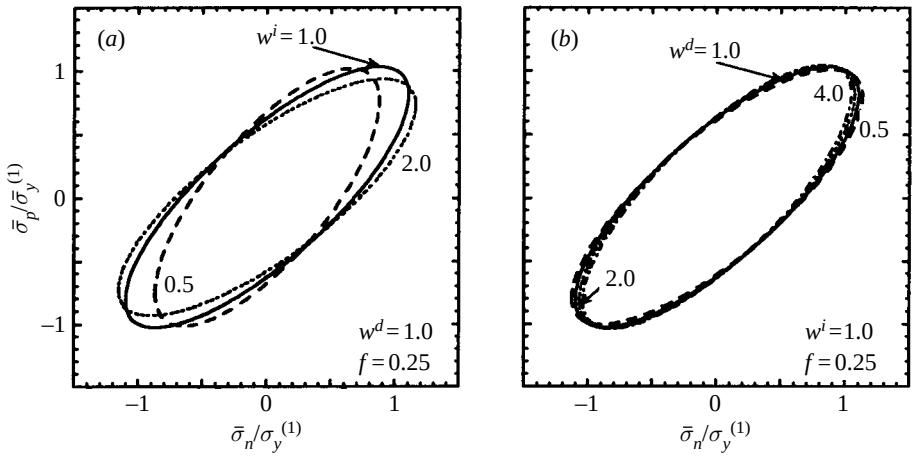

Figure 1. Yield surfaces for porous materials: (*a*) the aspect ratio w^{d} of the distribution is fixed, while the aspect ratio of the inclusions w^{i} is changed; (*b*) w^{d} is varied while w^{i} is fixed.

Detailed results have already been given by PCZ for the case where the aspect ratios of the distribution and the voids are the same ($w^{\mathrm{i}} = w^{\mathrm{d}}$). As already mentioned, the new feature of the present work is the ability to model composites with microstructures where these two aspect ratios may be different ($w^{\mathrm{i}} \neq w^{\mathrm{d}}$). For example, we may consider microstructures with a fixed aspect ratio for the distribution, but with varying aspect ratios for the voids, or vice versa. The $\bar{\sigma}_p - \bar{\sigma}_n$ cross-sections of the yield surface $\tilde{\Phi}(\bar{\sigma}) = 0$ (for porosity $f = 25\%$) are shown in figure 1 to demonstrate the effect of allowing the aspect ratio of the distribution of the voids to be different from those of the voids themselves. In figure 1*a*, we consider the yield surfaces of composites whose microstructure consists of an isotropic distribution of voids ($w^{\mathrm{d}} = 1$) and study the effect of void shape on the yield surface. It is seen that as the voids are made more oblate ($w^{\mathrm{i}} = 0.5$), the normal tensile yield strength $\bar{\sigma}_n$ tends to decrease while the transverse yield strength $\bar{\sigma}_p$ tends to increase. This can be understood in terms of the fact that as the voids become more oblate, the proportion of the matrix material in any transverse cross-section decreases (in an average sense), which results in a lower load-carrying capacity for normal tensile loading. The increase in $\bar{\sigma}_p$ can be explained in a similar way. It is also observed that making the voids prolate ($w^{\mathrm{i}} = 2$) has the opposite effect, although the effect is less marked. In figure 1*b*, the voids have a fixed shape ($w^{\mathrm{i}} = 1$) while the shape of the distribution is varied. It is observed that as the distribution becomes more oblate ($w^{\mathrm{d}} = 0.5$), $\bar{\sigma}_n$ increases while $\bar{\sigma}_p$ decreases. Again, this can be explained by the observation that a more oblate distribution results in more of the matrix material being present in any transverse cross-section. In this case also, it is noted that making the distribution prolate ($w^{\mathrm{d}} = 2,\ 4$) has the opposite effect ($\bar{\sigma}_n$ decreases and $\bar{\sigma}_p$ increases).

We observe that the effect of the shape of the distribution is, in general, the opposite of that of the shape of the voids. Thus, decreasing values of w^{i} tend to 'rotate' the yield surfaces toward the $\bar{\sigma}_p$ axis, whereas decreasing values of w^{d} tend to have the opposite effect, although the effect is much less marked in the second case. These observations are consistent with the findings of Ponte Castañeda & Willis (1995) for linear elastic systems. We recall that although the two aspect ratios can be allowed to be different from each other, there are some limitations on the range of values that one aspect ratio can take for a fixed value of the other aspect ratio. This arises

from the impenetrability restrictions on the 'security regions' of the voids (see Ponte Castañeda & Willis 1995). Finally, it should also be mentioned that the effect of the distribution is smaller than that of the shape of the voids. (A similar conclusion has been reached by Koplik & Needleman (1988) in the context of numerical simulations for periodic porous media.) This is to be expected since the effect of the distribution is of second order in the porosity, while shape effects are of first order. More detailed studies of the effect of the distribution on the yield strength of composites have been performed, but they will not be shown here for brevity.

(*b*) *Evolution of the microstructure*

We consider a porous material that is initially made up of an isotropic distribution of spherical voids in a perfectly plastic matrix with a porosity of 15% and which is subjected to axisymmetric strain-controlled loading of the type

$$\bar{\sigma}_{11} = \bar{\sigma}_{22} = \beta\bar{\sigma}_{33}, \quad \bar{\sigma}_{ij} = 0 \text{ if } i \neq j, \quad \bar{D}_{33} = \xi, \tag{2.2}$$

where β and ξ are prescribed constants. The instantaneous constitutive equations for the composite are then given by the following expression (see part I for details):

$$\bar{D}_{ij} = \frac{1}{H}\frac{\partial\tilde{\Phi}}{\partial\bar{\sigma}_{ij}}\frac{\partial\tilde{\Phi}}{\partial\bar{\sigma}_{kl}}\dot{\bar{\sigma}}_{kl}, \tag{2.3}$$

where the hardening rate H is obtained from the expression

$$H = -\left[(1-f)\frac{\partial\tilde{\Phi}}{\partial f}\frac{\partial\tilde{\Phi}}{\partial\bar{\sigma}_{kk}} + w^{\mathrm{i}}\frac{\partial\tilde{\Phi}}{\partial w^{\mathrm{i}}}\left\{(2a_5 - a_1)\frac{\partial\tilde{\Phi}}{\partial\bar{\sigma}_{11}} + (a_2 - a_6)\frac{\partial\tilde{\Phi}}{\partial\bar{\sigma}_{33}}\right\} + \cdots + w^{\mathrm{d}}\frac{\partial\tilde{\Phi}}{\partial w^{\mathrm{d}}}\left(\frac{\partial\tilde{\Phi}}{\partial\bar{\sigma}_{33}} - \frac{\partial\tilde{\Phi}}{\partial\bar{\sigma}_{11}}\right)\right], \tag{2.4}$$

while the yield function $\tilde{\Phi}$ is given by (2.1).

As mentioned earlier, when such a composite is subjected to axisymmetric loads of the type (2.2), the relevant microstructural variables are the porosity (f), the aspect ratio of the voids (w^{i}) and the aspect ratio of the distribution of the voids (w^{d}). The evolution equations for these variables may be written as

$$\dot{f} = (1-f)\bar{D}_{kk}, \tag{2.5}$$

$$\dot{w}^{\mathrm{i}} = w^{\mathrm{i}}[(2a_5 - a_1)\bar{D}_{11} + (a_2 - a_6)\bar{D}_{33}], \tag{2.6}$$

and

$$\dot{w}^{\mathrm{d}} = w^{\mathrm{d}}[\bar{D}_{33} - \bar{D}_{11}], \tag{2.7}$$

where the a_i are the components of the strain-rate concentration tensor $\boldsymbol{A}^{(2)}$, given in the Appendix of part I. It is recalled that $\boldsymbol{A}^{(2)}$, in this case, depends on all the relevant microstructural variables ($\boldsymbol{A}^{(2)} = \boldsymbol{A}^{(2)}(f, w^{\mathrm{i}}, w^{\mathrm{d}})$), but not on the material properties. To obtain the effective response of the composite, the evolution equations (2.5), (2.6) and (2.7) are solved in conjunction with the instantaneous constitutive equation (2.3), along with expression (2.4) for the hardening rate.

The effect of the evolution of the pore shape on the effective response of porous materials has already been discussed by PCZ. The reader is referred to that reference for more details and, in particular, for a detailed study of the effect of triaxiality. Here, we recall that the effect of changes in the shape of the voids can be of the same order as that of the changes in porosity, at least for low values of the triaxiality.

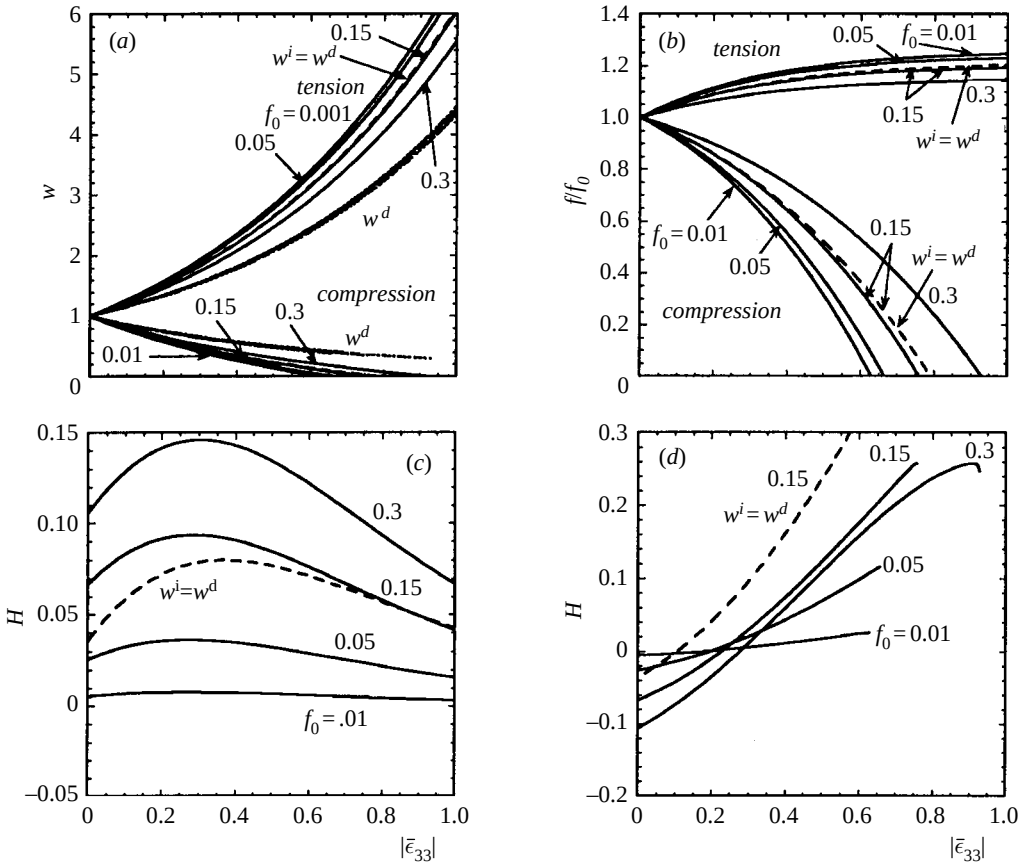

Figure 2. Effect of initial porosity on the evolution of the microstructure and on the effective response of the porous material under uniaxial tension and compression: (*a*) the evolution of the aspect ratios w^{i} (continuous lines) and w^{d} (short-dash lines) for different initial porosities; (*b*) the evolution of the porosity f; (*c*) the evolution of the effective hardening rate H for uniaxial tension; (*d*) the evolution of the effective hardening rate H for uniaxial compression (long dash lines correspond to simplified theory of PCZ).

In addition, it was observed in PCZ that changes in the shape of the voids can significantly affect the evolution of the porosity and that the overall response of the composite can become significantly anisotropic during a finite deformation process. In this work, we concentrate on the effect of the evolution of the distribution of the voids on the effective response of the composite, as it is subjected to finite deformations. In particular, in this section, we study the cases where the composites are subjected to uniaxial tension and compression ($\beta = 0$ in (2.2)).

In figure 2, plots are shown for the evolution of the aspect ratios of the voids (w^{i}) and their distribution (w^{d}), as well as for the porosity (f) and effective hardening rate (H), as functions of the logarithmic strain in the axial direction ($\bar{\varepsilon}_{33} = \int_0^t \bar{D}_{33}\,\mathrm{d}t = \xi t$) for porous materials with an initially isotropic distribution of spherical pores, at various values of the initial porosity f_0. It is seen, from figure 2*a*, that w^{i} (shown as continuous lines) changes at a faster rate than w^{d} (shown as short-dash lines), for both uniaxial tension and compression. This may be attributed to the fact that the deformation in this case is concentrated in the (softer) voids. For both tension and compression, we note that w^{d} evolves in essentially the same way for different initial

porosities. This results from the fact that the evolution of w^{d} is controlled by the average rate of deformation in the composite whose components are not significantly affected by the value of f_0 (recall that $\bar{D}_{33}$ is a prescribed constant). On the other hand, it is observed that the evolution of w^{i} depends considerably on the initial porosity. This can be understood in terms of the fact that the evolution of w^{i} is controlled by the average rate of deformation in the voids and this is a function of the porosity. Also plotted, for comparison, are the evolution curves (shown as long-dash lines) for the aspect ratio of the voids obtained by PCZ for $f_0 = 0.15$, assuming that the aspect ratio of the distribution evolves in precisely the same fashion as the aspect ratio of the voids ($w^{\mathrm{d}} = w^{\mathrm{i}}$). It is observed that the evolution of w^{i} predicted in the two cases are almost identical, even at this relatively large value of f_0.

In figure 2*b*, plots are shown for the evolution of the porosity, f, normalized by the initial porosity, f_0, under uniaxial tension and compression for different initial values of f_0. For tension, it is seen that the porosity in each case increases and reaches a final value which depends on the initial porosity, with increasing f_0 leading to smaller final values of f/f_0. On the other hand, for compression, it is observed that the strain at which the porosity becomes zero is also a function of the initial porosity, with increasing f_0 resulting in an increase in the strain at which the porosity approaches zero. In particular, for $f_0 = 0.15$, the porosity approaches a finite value ($f \to 0.179$) for tensile loading, while it approaches zero at $\bar{\varepsilon}_{33} = 0.758$ for compressive loading. By comparing these predictions for $f_0 = 0.15$ with the corresponding predictions of PCZ (shown as long-dash lines) for tensile loading, it is seen that allowing the distribution of the voids to evolve independently of the shape of the voids makes the porosity evolve at a slower rate and also the final value of the porosity is slightly less than that predicted by PCZ ($f \to 0.181$). On the other hand, for compression, the new results show that the porosity decreases at a faster rate and approaches zero for an axial strain that is less by about 4% than that predicted by PCZ.

In figures 2*c*, *d*, plots of the effective hardening rate H as a function of $\bar{\varepsilon}_{33}$ are shown for different initial porosities, for uniaxial tension and compression, respectively. It is observed that for $f_0 = 0.01$, H is close to zero (for both tension and compression) corresponding to the limiting case of a homogeneous perfectly plastic material, while for larger porosities the behaviour is significantly different from that of a perfectly plastic material. Thus, for larger values of f_0, it is observed that, for tensile loading, H initially increases and then decreases, but remains positive throughout the deformation process, whereas, for compression, H is initially negative and then increases monotonously with increasing deformation to become positive. It is also observed that the amount of deformation required for the hardening rate to become positive, for compressive loading, increases slightly for larger values of f_0. Finally, it is seen that the response of the composite predicted by PCZ (shown in dash lines), for $f_0 = 0.15$, is qualitatively similar, although quantitatively different from that of the present model. In particular, for compression, allowing the aspect ratios of the distribution to evolve independently of the shape of the voids results in the hardening rate being negative for a larger amount of deformation. However, it should be emphasized that the effect of the distribution on the effective hardening rate is not as significant as that of the shape of the voids or of the porosity.

(*c*) *Discussion and comparisons with other works*

The purpose of this section is to compare the present model with other models and numerical simulations for porous ductile solids that have been presented in the

literature over the past 20 years. One of the first models for porous ductile (perfectly plastic) solids is due to Gurson (1977), who made use of the earlier analyses by McClintock (1968) and Rice & Tracey (1969) to account for the effect of porosity and its evolution on the constitutive response of porous ductile materials subjected to nearly *hydrostatic* loading conditions. The motivation for Gurson's work, as well as for its extensive applications in the literature, derives from its potential implications for ductile fracture. Among several works to investigate the evolution of void shape and size in porous power-law viscous solids, we may cite the articles of Budiansky *et al.* (1982) and Banks-Sills & Budiansky (1982), as well as the more recent works of Lee & Mear (1994) and Needleman *et al.* (1995). However, these works focused on the details of the evolution of a single void in an infinite matrix or a finite cell, but did not consider the implications of the evolution of the microstructure on the effective constitutive response of the porous solids.

As far as full constitutive models—incorporating the effects of void size, shape and their evolution on the effective response of porous materials—are concerned, there are basically two types currently available. The first type, due to Gologanu *et al.* (1993, 1994*a*), following the work of Lee & Mear (1992), constitutes an extension of the Gurson model for *perfectly plastic* porous solids, subjected to *axisymmetric* loading conditions. The second is the more general model of Ponte Castañeda & Zaidman (1994), which applies for general *nonlinearly viscous* porous solids, as well as general *triaxial* loading conditions, including axisymmetric and plane strain loading. Of course, the present work constitutes an extension of this second class of models to incorporate additionally the effect of the distribution of the voids and its evolution.

In an attempt to provide numerical corroboration for the predictions of our model, figures 3 and 4 provide plots of the evolution of the aspect ratio of the voids (w^{i}), porosity (f) and equivalent average stress ($\bar{\sigma}_{\mathrm{e}} = (1-\beta)\bar{\sigma}_{33}$) in a porous perfectly plastic material with an initially isotropic distribution of spherical voids, as functions of the equivalent strain, ($\bar{\varepsilon}_{\mathrm{e}}$), for three different triaxiality levels resulting in *prolate* ($X = \frac{1}{3}, \frac{2}{3}, 1$, where $X = (1+2\beta)/(3(1-\beta))$) and *oblate* ($X = -\frac{1}{3}, -\frac{2}{3}, -1$) pore shapes, respectively. The idea is to be able to compare these results with the FEM unit-cell computations of Gologanu *et al.* (1993, 1994*a*, *b*) (see also Koplik & Needleman (1988) for $X = 1$, 2 and 3). The results of Gologanu *et al.* (1994*b*) (which were scanned from *their* figures 2–7) are included in *our* figures 3 and 4. From these comparisons, the following conclusions may be drawn.

First, our results given in figures 3*a*–*c* (shown as continuous lines) for the evolution of the aspect ratio, porosity and stress, respectively, are in good qualitative agreement with the numerical results of Gologanu *et al.* (shown in figures 3*d*–*f* as long-dashed lines) for axisymmetric loading conditions resulting in *prolate* void shapes. However, significant quantitative differences may arise for sufficiently large strains, especially for the largest triaxiality value ($X = 1$). Consistent with the results of Gologanu *et al.* (see figure 3*f*), it can be seen from figure 3*c* that $\bar{\sigma}_{\mathrm{e}}$ increases for $X = \frac{1}{3}$, whereas it decreases for $X = \frac{2}{3}$ and 1. As pointed out by PCZ, this can be understood in terms of the fact that the porosity increases (see figure 3*b*), for $X = \frac{2}{3}$ and 1, thus providing a strong softening mechanism, whereas f levels off for $X = \frac{1}{3}$, resulting in slight overall hardening, as a consequence of the change in shape of the voids (see figure 3*a*).

Second, it is remarked that the numerical simulations predict a large drop in the stress, for $X = 1$, at a strain of about 40%, as a consequence of the fact that the strain localizes in the ligament between the voids, resulting in void coalescence (note

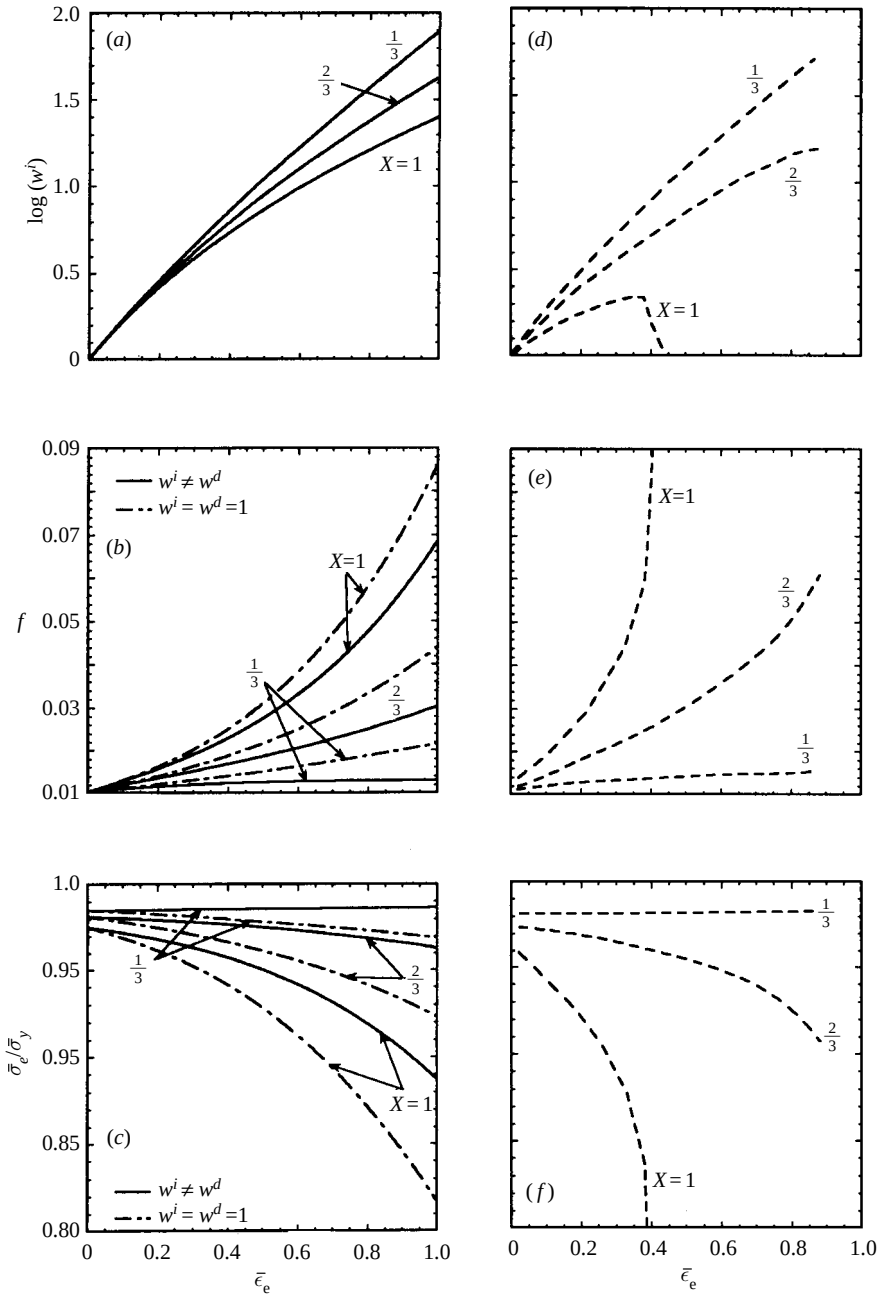

Figure 3. Comparison of the model predictions for the evolution of the microstructure and for the effective response of the porous materials with the unit-cell numerical results of Gologanu *et al.* (1994*b*). The initial value of the porosity is 1.04% and the material is subjected to axisymmetric loading conditions with three triaxiality levels leading to *prolate* void shapes. (*a*) and (*d*) give the evolution of the aspect ratio of the voids for the model and numerical predictions, respectively. (*b*) and (*e*) give the corresponding model and numerical predictions for the evolution of the porosity. (*c*) and (*f*) give the corresponding model and numerical predictions for the effective stress–strain relations. (Results are also shown in parts (*a*), (*b*) and (*c*) for the model assuming that the shape of the voids and their distribution remains fixed.)

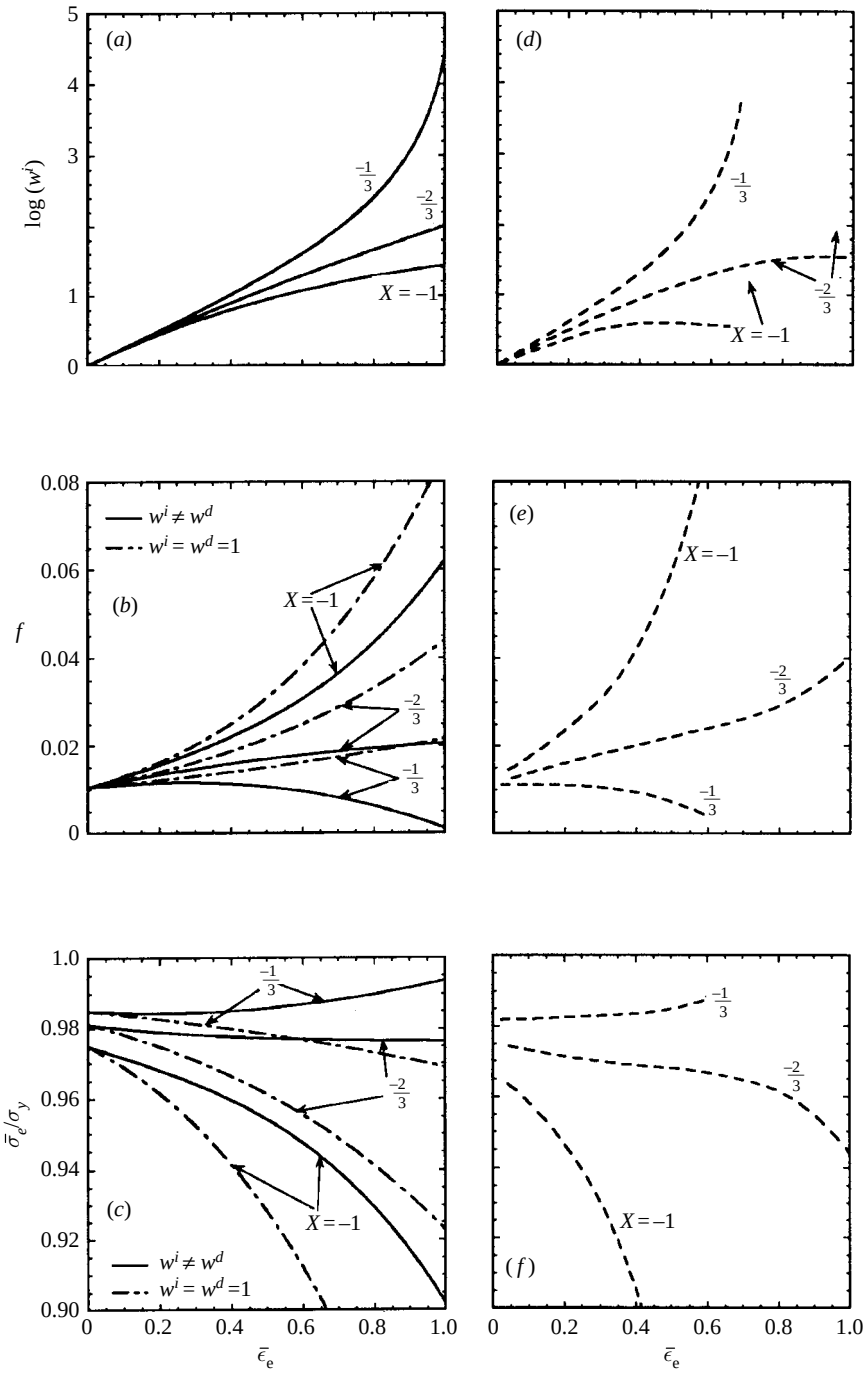

Figure 4. Same as in figure 3, but for triaxiality levels leading to *oblate* void shapes.

that the porosity undergoes a sharp increase at this point). Our model is not able to capture the details of these strongly nonlinear void-interaction effects, but it is able to provide some information as to the possible developments of such instabilities, in the following sense. The model predicts that the overall hardening rate (essentially,

the slope of the stress curve) for the porous composite is positive for $X = \frac{1}{3}$, but negative for $X = \frac{2}{3}$ and 1. As mentioned in PCZ, this suggests that the deformation for the first case will be stable, whereas that for the second case may be unstable. Thus, while the homogenized model is unable to capture the details of the instability development, it has the capability of predicting *whether* such instabilities may occur. Evidently, they seem to occur if the effective hardening rate is negative, but they are excluded if H is positive.

Third, in figures 3*a–c*, a comparison is also given between the predictions of the model with evolution of the porosity and the aspect ratios of the voids and distribution taken into account (continuous lines) and the corresponding predictions of the model with evolving porosity, but with fixed aspect ratios, $w^{\mathrm{i}} = w^{\mathrm{d}} = 1$ (dot-dashed lines). In part, the motivation for this comparison is that it has already been established (see PCZ) that the model with fixed $w^{\mathrm{i}} = w^{\mathrm{d}} = 1$ leads to predictions that are very similar to those of the Gurson model, at least for low-triaxiality levels. Thus, this type of comparison gives an idea of the types of errors that are introduced by any model, including the Gurson model, which neglects the change in shape of the voids (and distribution, to a lesser extent). For the specific types of loading depicted in figure 3, it appears that neglecting the changes in shape of the voids (and distribution) tends to overestimate the predicted increase in the porosity and, therefore, the drop in the load-carrying capacity of the porous solid. This is specially the case for $X = \frac{1}{3}$, where accounting for changes in the shape of the voids results in increasing stress, versus the opposite prediction when shape changes are neglected.

Similarly, for cases where the voids are subjected to axisymmetric loading resulting in *oblate* shapes ($X = -\frac{1}{3}$, $-\frac{2}{3}$ and -1), the following observations may be made by comparing the predictions of our model (figures 4*a–c*) with the corresponding predictions of the numerical simulations of Gologanu *et al.* (figures 4*d–f*). First, the predictions of our model are in fairly good qualitative agreement with the numerical predictions, although quantitative differences arise for sufficiently large strains. Once again, the differences are significant for the larger triaxiality values ($X = -\frac{2}{3}$ and -1) and can be attributed to the void coalescence phenomenon in the numerical simulations, resulting in sharper changes in the porosity and overall stress. On the other hand, for the low-triaxiality value ($X = -\frac{1}{3}$), the predictions of our model and of the numerical simulation are in excellent agreement, with the porosity first increasing and then decreasing, leading to the opposite behaviour for the overall stress.

Second, although initially negative (only slightly so), the effective hardening rate of the porous material for $X = -\frac{1}{3}$ turns around and becomes positive. This prediction from our model suggests that for this level of triaxiality the overall deformation should be stable, which is what is observed in the numerical simulations. On the other hand, for the higher values of the triaxiality, the model predicts negative overall hardening rates, suggesting the possible development of instabilities, which, as already mentioned, are observed in the numerical simulations at sufficiently high strains. Thus, it is found that the model provides correct qualitative predictions, including an indication of *whether* the development of shear instabilities (associated with void coalescence) is possible.

Third, in figures 4*a–c*, comparisons are also given between the predictions of the model (continuous lines) and the corresponding predictions with evolving porosity, but with fixed aspect ratios, $w^{\mathrm{i}} = w^{\mathrm{d}} = 1$ (dot-dashed lines). For the specific types of loading depicted in figure 4, it appears that neglecting the changes in shape of the

voids (and distribution) tends to overestimate the increase in porosity, as well as the drop in the load-carrying capacity for the porous solid, especially for $X = -\frac{1}{3}$.

Comparisons for the evolution of the microstructural variables have also been carried out with the dilute results of Lee & Mear (1994) (see also Budiansky *et al.* 1982). While the results of Lee & Mear, for power-law viscous porous materials, show an increasingly strong dependence on the nonlinearity for increasing values of the triaxiality, the predictions of the model for the evolution of the microstructural variables are rather insensitive to the nonlinearity (see Kailasam & Ponte Castañeda 1995), and hence not appropriate for large triaxialities, as already mentioned in PCZ. (Note that void shape change effects are relatively unimportant for sufficiently large triaxialities.) However, the model is found to be in good qualitative agreement with the numerical predictions of Lee & Mear (1994), for small to moderate triaxiality ($|X| \leqslant \frac{4}{3}$). In particular, the model captures the saturation of porosity for uniaxial tensile loading (see also Needleman *et al.* 1995) and the much faster collapse of the voids for uniaxial compressive loading. Thus, the model predicts complete void collapse, for dilute porosity levels, at an overall strain of about 60% (it increases with initial porosity; see figure 2*b*) whereas the simulations of Lee & Mear (1994) (see also Banks-Sills & Budiansky 1982) lead to a corresponding value between 50 and 65% depending on the specific nonlinearity. As noted by PCZ and also by Lee & Mear (1994), this level is significantly more realistic than the corresponding prediction of the Gurson model with spherical inclusions (over 200%), and thus in closer agreement with experiment (see, for example, daSilva & Ramesh 1991; Wang & Richmond 1992).

We conclude this section with two comments. First, we note that the limitations of the model in terms of underestimating the dependence of the evolution of the microstructural variables on the nonlinearity, in particular for large triaxialities, appears to be associated with the intrinsic limitations of the nonlinear homogenization procedure, rather than with errors associated with the modelling of the evolution phenomenon itself. Therefore, it is probable that improvements in the nonlinear homogenization procedure may alleviate these current limitations of the model. Second, it was made clear in the previous section that the effect of changes in the distribution of the voids are fairly small for porous materials, and therefore it is unlikely that such effects would be detectable by numerical simulation or experiment. However, as we will see in the next section, these effects can become relatively important for particle-reinforced composites when the particles are sufficiently strong.

3. Application to two-phase composites with perfectly plastic phases

(*a*) *Effective yield functions*

In this section, we obtain estimates for the effective yield functions of two-phase composites where both phases—the inclusions and the matrix—are perfectly plastic. For such a composite, the effective yield surface is given by expression (6.8) of part I. Here, we consider composites with microstructures that initially consist of isotropic distributions of spherical inclusions; they are subjected to axisymmetric loads where the only non-zero transversely isotropic incompressible invariant of the stress is $\bar{\tau}_d = (\bar{\sigma}_n - \bar{\sigma}_p)/\sqrt{3}$. It is noted that, in this case, because of incompressibility, the hydrostatic stress is indeterminate and the volume fractions of the phases remain fixed. Therefore, the relevant microstructural variables are the aspect ratio of the inclusions w^{i} and the aspect ratio of the distribution w^{d}. The effective yield

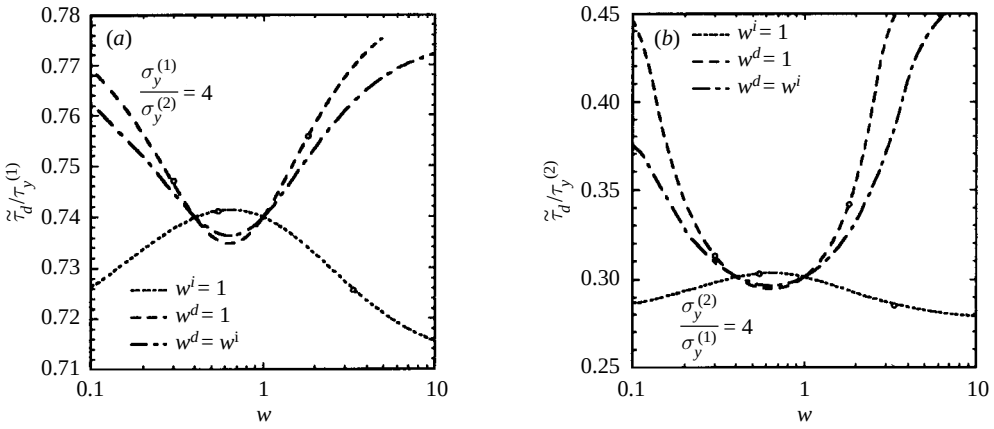

Figure 5. The effect of the aspect ratios of the distribution and the inclusions on the single-mode yield strength $\tilde{\tau}_d$ of two-phase composites with perfectly plastic phases, with an inclusion volume fraction $c^{(2)} = 30\%$: (*a*) the matrix is the harder phase; (*b*) the inclusions are the harder phase.

function of the composite is then given by the expression

$$\tilde{\Phi}(\bar{\sigma}) = (\bar{\tau}_d/\tilde{\tau}_d)^2 - 1 = 0, \tag{3.1}$$

where the single-mode axisymmetric yield stress $\tilde{\tau}_d$ is in turn given by the expression

$$\left(\frac{\tilde{\tau}_d}{\tau_y^{(1)}}\right)^2 = \min_{y \geqslant 0}\left[\left(\frac{1}{m_1(y)}\right)\left(c^{(1)} + c^{(2)}\frac{z^2}{y}\right)\right], \tag{3.2}$$

where $\tau_y^{(1)} = \sigma_y^{(1)}/\sqrt{3}$ is the yield strength in shear of the matrix; $c^{(1)}$ and $c^{(2)}$ are the volume fractions of the matrix and the inclusions, respectively; $z = \sigma_y^{(2)}/\sigma_y^{(1)}$ is the ratio of the yield strengths of the inclusions and the matrix; and the expression for m_1, as a function of w^{i}, w^{d} and y, is given in the Appendix of part I.

Here, we study the effect of the aspect ratio of the inclusions (w^{i}) and their distribution (w^{d}) on the axisymmetric-mode yield strength $\tilde{\tau}_d$ of the composite. Results for the case where the aspect ratios of the inclusions and the distributions are the same ($w^{\mathrm{i}} = w^{\mathrm{d}}$) have already been given by Ponte Castañeda & Zaidman (1996). Here, we shall concentrate on composites with microstructures where the two aspect ratios are allowed to be different ($w^{\mathrm{i}} \neq w^{\mathrm{d}}$). For illustrative purposes, we choose the composite to be such that the two phases have yield strengths in the ratio four, with inclusion volume fraction $c^{(2)} = 0.3$. In one case, we choose the inclusions to be harder so that $\sigma_y^{(2)}/\sigma_y^{(1)} = 4$ and in the other case the matrix to be harder so that $\sigma_y^{(1)}/\sigma_y^{(2)} = 4$.

In figures 5*a*, *b*, corresponding to harder matrix and inclusion phases, respectively, plots of the yield strength $\tilde{\tau}_d$ are shown for three cases. In the first case, w^{i} is fixed and w^{d} is allowed to vary; in the second, w^{d} is fixed and w^{i} is allowed to vary; and in the third, $w^{\mathrm{i}} = w^{\mathrm{d}}$ is allowed to vary. It is observed that the effects of the aspect ratios on the yield strength of the composite are similar, both when the inclusions are softer and when the matrix is softer. However, it is noted that these effects are more pronounced when the inclusions are harder. Irrespective of whether the inclusions are softer or harder than the matrix, when $w^{\mathrm{i}} = 1$ and w^{d} is varied, it is observed that $\tilde{\tau}_d$ reaches a maximum for values of w^{d} slightly less than one. On the other hand when w^{d} is fixed, we note that $\tilde{\tau}_d$ achieves a minimum for values of w^{i} slightly less than one. When $w^{\mathrm{d}} = w^{\mathrm{i}}$, the predictions of the yield strength $\tilde{\tau}_d$ are in

between those of the two earlier cases. This can be explained by noting that, as for the porous composites, here also the effect of particle-distribution shape is roughly the opposite of that of the particle shape, but less significant in relative terms. This causes the yield stress when $w^{\mathrm{d}} = w^{\mathrm{i}}$ to lie in between the two other curves, but closer to the fixed w^{d} curves than to the fixed w^{i} curves. It is emphasized that the effect of the distribution on the yield strength is, as expected, smaller than that of the aspect ratio of the inclusions. This is due to the fact that distribution effects are of second order in the volume fraction of the inclusions while the effect of shape of the inclusions is of first order.

Finally, it is recalled that the hypothesis of 'impenetrability' of the inclusions (see Ponte Castañeda & Willis 1995) imposes certain restrictions on the values that w^{i} (w^{d}) can take for a fixed value of w^{d} (w^{i}). The results shown in figure 5 are thus rigorously valid only in this range, the limits of which are demarcated by open circles on the curves. It is also noted that numerical results for particle-reinforced composites with periodic microstructures have been given by Bao *et al.* (1991), making use of finite element computations on cylindrical unit cells. These results are roughly consistent with our findings, except that the numerical predictions are more sharply dependent on the volume fraction and aspect ratios of the inclusions and distribution. This is presumably due to the periodicity assumption in the numerical results, which leads to stronger interactions than that for the Hashin–Shtrikman microstructures assumed in this work.

(*b*) *Evolution of the microstructure*

In this section, we consider the application of the model to analyse the evolution of the microstructure and its effect on the overall response of two-phase incompressible composites with perfectly plastic phases as they are subjected to axisymmetric loading. Due to incompressibility, the volume fractions of inclusions ($c^{(2)}$) and the matrix ($c^{(1)}$) remain fixed throughout the deformation process. In addition, it suffices to specify the (constant) axial strain rate $\bar{D}_{33} = \xi$, so that $\bar{D}_{11} = \bar{D}_{22} = -\frac{1}{2}\bar{D}_{33}$. Recalling that the stress components $\bar{\sigma}_{33}$ and $\bar{\sigma}_{11} = \bar{\sigma}_{22}$ are indeterminate to within a hydrostatic pressure, we choose, for convenience $\bar{\sigma}_{11} = \bar{\sigma}_{22} = 0$. Here, we will consider composites that are initially made up of an isotropic distribution ($w^{\mathrm{d}} = 1$) of spherical inclusions ($w^{\mathrm{i}} = 1$) with inclusion volume fraction $c^{(2)} = 0.3$. Then, for the loading conditions considered (prescribed $\bar{D}_{33}$), the relevant microstructural variables are w^{i} and w^{d}. The evolution equations for these variables can be written as (using $\bar{D}_{11} = \bar{D}_{22} = -\frac{1}{2}\bar{D}_{33}$)

$$\dot{w}^{\mathrm{i}} = w^{\mathrm{i}}[\tfrac{1}{2}a_1 + a_2 - 2a_5]\bar{D}_{33}, \tag{3.3}$$

and

$$\dot{w}^{\mathrm{d}} = \tfrac{3}{2}w^{\mathrm{d}}\bar{D}_{33}, \tag{3.4}$$

where the a_i are the components of the strain-rate concentration tensor $\boldsymbol{A}^{(2)}$ and are given in the Appendix of part I. It is emphasized that in these expressions for the a_i, the optimized value of y, obtained from the optimization in (3.2), must be used (recall that $\boldsymbol{A}^{(2)} = \boldsymbol{A}^{(2)}\ (w^{\mathrm{i}}, w^{\mathrm{d}}; \hat{y})$, where $\hat{y}$ is the optimal value of y). The instantaneous constitutive equation for the incompressible composite is given by (2.3) where the expression for the hardening rate H can be written in the form

$$H = -\left[w^{\mathrm{i}}\frac{\partial\tilde{\Phi}}{\partial w^{\mathrm{i}}}(a_1 + 2a_2 - 4a_5) + 3w^{\mathrm{d}}\frac{\partial\tilde{\Phi}}{\partial w^{\mathrm{d}}}\right]\frac{1}{\bar{\sigma}_{33}}, \tag{3.5}$$

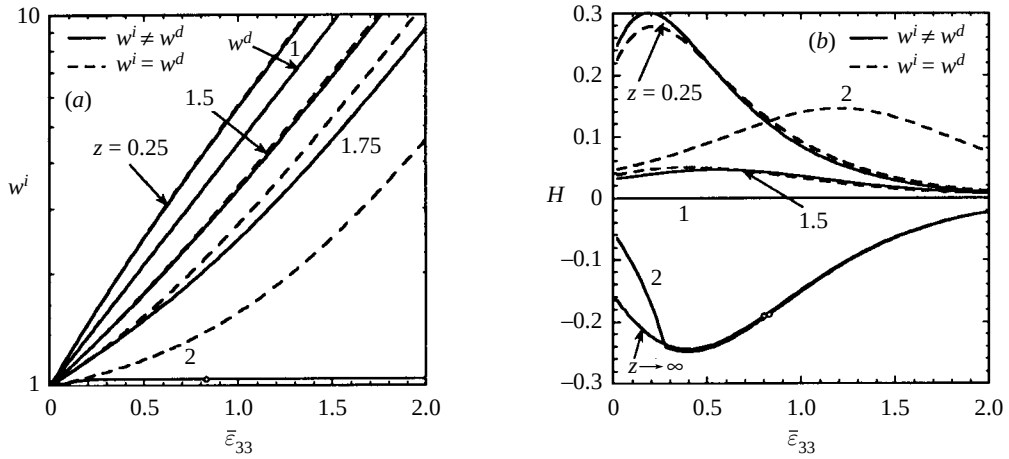

Figure 6. Evolution curves for two-phase composites with an initially isotropic distribution of spherical perfectly plastic inclusions (with volume fraction $c^{(2)} = 30\%$) in a perfectly plastic matrix when subjected to uniaxial tension ($\bar{D}_{33} > 0$) for different values of the yield strength ratio z: (*a*) evolution of the aspect ratio w^{i} (and w^{d}); (*b*) evolution of the hardening rate H. Corresponding results of ZPC ($w^{\mathrm{i}} = w^{\mathrm{d}}$) are shown for comparison.

and the yield function $\tilde{\Phi}$ is given by (3.1). It is also observed that when we choose $\bar{\sigma}_{11} = \bar{\sigma}_{22} = 0$, the yield condition (3.1) specializes to

$$\bar{\sigma}_{33} = \sqrt{3}\tilde{\tau}_d. \tag{3.6}$$

The effects of changes in the shape of the inclusions on overall response for this class of composites have been considered in some detail by ZPC. In the present work, we shall therefore emphasize the corresponding effect of the distribution and its evolution. In particular, we will consider the case of rigid inclusions, where the shape of the inclusions remains fixed, in order to isolate the effects of the distribution on the effective response of composites. When $\bar{D}_{33}$ is prescribed, the evolution equation (3.4) for w^{d} is easily solved, but since the a_i in equation (3.3) need to be evaluated at the optimal $\hat{y}$, the evolution equation (3.3) for w^{i} requires the solution of (3.2) for $\hat{y}$. Having found the history of w^{d} and w^{i}, as well as $\hat{y}$ as a function of these variables, the history of $\bar{\sigma}_{33}$ follows from (3.6) with (3.2).

Next, we consider the application of the model to uniaxial *tensile* ($\bar{D}_{33} > 0$) and *compressive* ($\bar{D}_{33} < 0$) loading. In figure 6*a* plots are given for the evolution of w^{i} and w^{d} as functions of $\bar{\varepsilon}_{33} = \xi t$ for uniaxial *tensile* loading and for different values of the yield strength ratio z. The aspect ratio of the distribution evolves along the curve $z = 1$, which corresponds to identical materials for both phases, for all values of z. This is as expected, since the evolution of w^{d} is controlled by the average rate of deformation in the composite which is a constant in this case; in fact, $w^{\mathrm{d}} = \exp(\frac{3}{2}\bar{\varepsilon}_{33})$. It is seen that for $z < 1$ (inclusions are softer than the matrix) w^{i} changes faster than w^{d}, corresponding to the deformation being concentrated in the inclusions. On the other hand, for $z > 1$ (harder inclusions) w^{i} changes at a slower rate than w^{d} ($z = 1.5$, 1.75). For sufficiently large z (e.g. $z = 2$) the inclusions initially begin to change shape, but after a certain amount of deformation, they 'lock up' and behave like rigid particles while the distribution continues to evolve (along the curve $z = 1$) as a consequence of the deformation being concentrated in the softer matrix phase.

For purposes of comparison, we also show in figure 6*a* the results of ZPC for the evolution of w^{i}, assuming that the aspect ratio of the distribution evolves just

like the aspect ratio of the inclusions. It is noticed that the evolution curves for w^{i} predicted in the two cases are almost identical for $z < 1$. This is because, for softer inclusions, the deformation is localized in the inclusions and the change in shape of the inclusions is then known to be dominant. Therefore, the change in the distribution does not affect the evolution of the shape of the inclusions significantly. When the inclusions are harder than the matrix ($z > 1$), greater differences are observed in the two predictions for the evolution of w^{i}. This is because the deformation is now concentrated in the matrix, so that the inclusions change shape at a slower rate, which makes the effect of the distribution more significant in relative terms. In particular, for $z = 2$, the two predictions for the evolution of w^{i} are very different. As mentioned earlier, when the distribution effects, which are now dominant, are taken into account, the inclusions lock up after a certain amount of deformation, while the corresponding results of ZPC do not exhibit lock up of the inclusions. It is noted that for values of $z > 2$, when distribution effects are taken into account, the inclusions effectively behave like rigid particles, while the aspect ratio of the distribution continues to evolve along the curve $z = 1$. At this point, it is appropriate to recall that the hypothesis of impenetrability of the inclusions places some restrictions on the values that the aspect ratios may take and that these results are rigorously valid only while the hypothesis is satisfied. The aspect ratios beyond which the results are not rigorously valid are identified by open circles on the evolution curves.

In figure 6*b* plots are shown for the evolution of the effective hardening rate H as a function of the tensile axial strain $\bar{\varepsilon}_{33}$. For the case where the inclusions are softer than the matrix (e.g. $z = 0.25$), it is seen that H is always positive. This is because the yield strength $\tilde{\tau}_d$, and hence the axial stress, ($\bar{\sigma}_{33} = \sqrt{3}\tilde{\tau}_d$), increases as w^{i} increases from its initial value of one (see figure 5*a*). It is also seen from figure 5*a* that an increase in the aspect ratio of the distribution causes $\tilde{\tau}_d$ to decrease, but as mentioned earlier, the shape effects are dominant, when the inclusions are softer than the matrix. As a consequence, the axial stress $\bar{\sigma}_{33}$ increases, and hence the hardening rate is positive. The hardening-rate curves for values of z up to 1.75 can also be explained in a similar manner because the shape effects continue to dominate over the distribution effects. However, for even larger values of z (e.g. $z = 2$) the distribution effects become dominant and the hardening becomes negative. (Note that the sudden change in the hardening curve at $\bar{\varepsilon}_{33} = 0.27$ is a consequence of the 'locking up' of the inclusions.) For the limiting case of rigid inclusions ($z = \infty$), as noted earlier, w^{d} continues to increase, although w^{i} does not undergo any change. This increase in w^{d} causes the axial stress to decrease which results in the hardening rate being negative throughout the deformation process. (Note that the curves for $z = 2$ and ∞ are almost identical, after lock up of the inclusions in the first case.)

Also shown in figure 6*b*, for the sake of comparison, are the results of ZPC (shown in dash lines), where the constraint $w^{\mathrm{i}} = w^{\mathrm{d}}$ was implicitly enforced throughout the deformation process. As expected, for small values of z, the differences between the improved model accounting for independent changes in the distribution of the particles and the earlier model with $w^{\mathrm{i}} = w^{\mathrm{d}}$ are relatively small. However, for sufficiently large values of z *qualitatively* different predictions are obtained for the two models. Thus, for $z = 2$, when $w^{\mathrm{i}} = w^{\mathrm{d}}$ increases, it is seen from figure 5*b* that the axial stress increases, which causes the hardening rate to be positive throughout the deformation process, which is in contrast with the predictions of the model incorporating distribution effects. Similarly, for the case where the inclusions are rigid, the model of ZPC predicts that the microstructure does not evolve with deformation, as

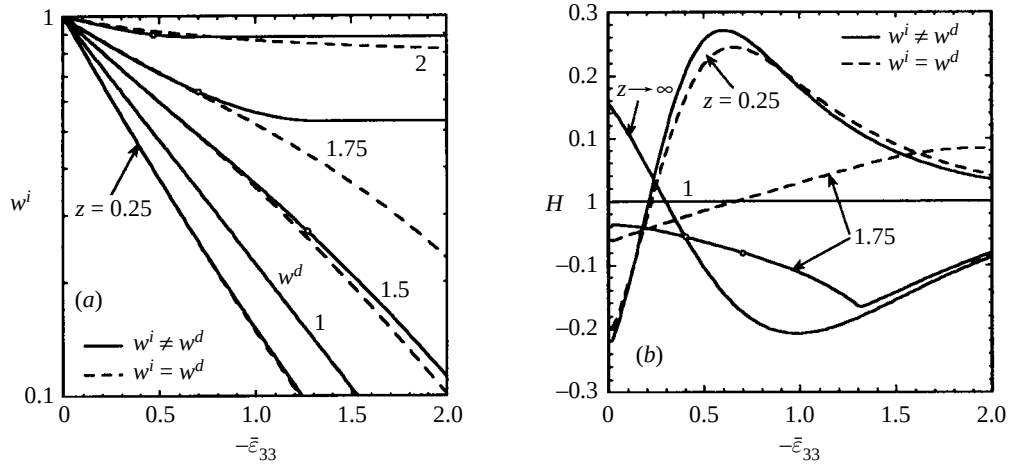

Figure 7. Evolution curves for two-phase composites with an initially isotropic distribution of spherical perfectly plastic inclusions (with volume fraction $c^{(2)} = 30\%$) in a perfectly plastic matrix when subjected to uniaxial compression ($\bar{D}_{33} < 0$) for different values of the yield strength ratio z: (a) evolution of the aspect ratio w^{i} (and w^{d}); (b) evolution of the hardening rate H. Corresponding results of ZPC ($w^{\mathrm{i}} = w^{\mathrm{d}}$) are shown for comparison.

a result of which the axial stress remains constant (corresponding to zero hardening rate). On the other hand, more realistically, the improved model takes into account the changes in the distribution of the particles, and predicts that the axial stress decreases with increasing deformation (corresponding to H being negative). These contrasting predictions provide a dramatic example of the fact that, for sufficiently hard inclusions, the effect of allowing the aspect ratio of the distribution to evolve as an independent variable on the overall response of the composite can be very important.

Next, we consider the evolution of the microstructure as the composite is subjected to uniaxial *compressive* loading such that $\bar{D}_{33} < 0$. As before, incompressibility results in $\bar{D}_{11} = \bar{D}_{22} = -\frac{1}{2}\bar{D}_{33}$ and we choose $\bar{\sigma}_{11} = \bar{\sigma}_{22} = 0$. Shown in figure 7$a$ are the evolution curves for the aspect ratios w^{i} and w^{d} for different values of z. We note that, as before, w^{d} evolves along the curve $z = 1$ for all values of z. Also, similar to the results for the case with $\bar{D}_{33} > 0$, we see that w^{i} changes faster when the inclusions are softer ($z < 1$), while for the case where $z > 1$ the deformation is concentrated in the matrix and w^{d} evolves at a faster rate. It is also noted that for sufficiently large values of z ($z \geqslant 1.75$) the inclusions lock up after a certain amount of deformation. For the case of rigid inclusions, it is clear that while the inclusions themselves undergo no change, their distribution continues to change with deformation.

As was the case for $\bar{D}_{33} > 0$, there are no significant differences between the new and ZPC (with $w^{\mathrm{i}} = w^{\mathrm{d}}$) predictions for the case where the inclusions are softer than the matrix. As the inclusions become harder, the distribution effects begin to influence the evolution of w^{i}, although for the range where the results are rigorously valid (demarcated by the open circles) the differences between the two sets of predictions are not very significant. For $z = 1.75$, when distribution effects are taken into account, the new predictions give lock up of the inclusions after a certain amount of deformation, while the old ZPC predictions do not show lock up of the inclusions. However, for $z = 2$, the new and old predictions appear to be in

fairly good agreement, even for large deformations, both predicting relatively small changes in w^{i} before lock up.

In figure 7*b* the hardening rate H is shown as a function of the axial strain for different values of z. It is seen that for $z = 0.25$, H is initially negative but becomes positive after a certain amount of deformation. This can be explained by noting that as w^{i} decreases from its initial value of one, the axial stress decreases in magnitude (see figure 5*a*) until it reaches a minimum value and thereafter begins to increase. (Note that the effect of the distribution is opposite to that of the shape of the inclusions, but is much smaller in this case.) For $z = 1.75$, H is found to be negative throughout the deformation process. This can be explained by noting that shape effects dominate initially, which causes the axial stress to decrease with decreasing w^{i}, despite the opposing effect of w^{d} to increase the axial stress. As the deformation progresses, the continued decrease in w^{d} beyond its critical value (see figure 5*b*) causes the axial stress to decrease (although at a slower rate), despite the opposing effect of w^{i}, because the particles lock up and the distribution effects take control. For the case of rigid inclusions, there is no change in the shape of the inclusions and hence the effects of changes in the distribution can be isolated. Thus, the axial stress initially increases with decreasing w^{d} but, beyond the critical value of w^{d}, further decreases in w^{d} cause the axial stress to decrease. This is reflected by the hardening rate initially being positive and negative thereafter.

It can also be seen from figure 7*b* that, for all values of z, the corresponding predictions of ZPC assuming that $w^{\mathrm{i}} = w^{\mathrm{d}}$ for the hardening rate are initially negative and then positive. Thus, the differences between the two sets of predictions are not significant for small values of z, but as the inclusions become harder, and therefore deform less, the differences between the predictions become important. In the limiting case of rigid inclusions, the inclusions do not undergo any change in their shape and hence the model of ZPC predicts that the hardening rate remains zero throughout the deformation process. On the other hand, as mentioned earlier, the improved model predicts that the hardening rate is initially positive but becomes negative with subsequent deformation. It is thus seen that, in this case also, the effect of the distribution becomes significant when the inclusions are sufficiently hard. This demonstrates the need to take into account the evolution of the distribution at least for the case where the inclusions are harder that the matrix.

Finally, we recall that the model is accurate only when the aspect ratios of the inclusions and the distribution are within the range prescribed by the hypothesis of impenetrability of the inclusions. In particular, for the case where the inclusions are rigid, this has important ramifications. As the composite undergoes finite deformation, the distribution of the rigid inclusions evolves—the aspect ratio increases in tension and decreases in compression—which suggests that the rigid inclusions may come into contact beyond a certain amount of deformation. Due to the incompressibility of the matrix, this would result in a marked increase in the strength of the composite. The model, in its present form, is unable to capture these effects because of the restrictions mentioned earlier. However, it must be noted that these restrictions arise from limitations of the homogenization procedure for the linear comparison composite. This leads to the suggestion that more general models could be developed by making use of improved linear homogenization results, incorporating more realistic statistics for the distribution of the inclusions.

In addition, we remark that in spite of the availability of several works (e.g. Bao *et al.* 1991) that have been devoted to the understanding particle reinforcement in

metal matrix composites, no work appears to have been carried out to examine the effect of microstructure evolution in the context of particle-reinforced solids. Because of this, comparisons with other models, or with numerical simulations are not possible at this time. There is, however, the work of Hom & McMeeking (1991) who considered the problem of a rigid particle, embedded in a cubic cell of a perfectly plastic material, subjected to uniaxial tension (and simple shear). Although these authors did not consider in any detail the evolution of the distribution of the particles (i.e. the change in shape of the unit cell) they presented plots for the uniaxial tensile stress as a function of the strain (their figure 4). There, for $f = 0.219$, it can be seen that yield stress in the composite appears to decrease initially (for small strains in the plastic domain) before increasing for larger strains. The initial decrease in the yield stress would be consistent with the predictions of our model, shown in figure 6*b*, which shows a negative hardening rate for rigidly reinforced composites subjected to uniaxial tension. On the other hand, the increase in the yield stress observed in the numerical results for large enough strains could be a consequence of the stronger particle interactions that would be expected for a composite with periodic microstructures, as opposed to the Hashin–Shtrikman type of microstructures implicit in our model.

4. Concluding remarks

Part I of this work was concerned with the development of constitutive models for two-phase nonlinear composites with particulate microstructures. The models, which are capable of taking into account the evolution of the microstructure when the composites are subjected to finite deformations, consist of two parts: instantaneous constitutive equations for the nonlinear composite and evolution equations for appropriate internal variables which characterize the microstructure at every instant. For simplicity, general triaxial loading conditions (with fixed axes) were considered thus reducing the number of the relevant microstructural variables to five: two aspect ratios for the ellipsoidal inclusions; two aspect ratios for the ellipsoidal distributions of the inclusions and the volume fraction of the inclusions. Evolution equations for these variables were then developed, which when solved in combination with the instantaneous constitutive equations provide a complete characterization of the effective response of the composite.

This part of the work was concerned with the application of the model to study the behaviour of two sample composite systems—porous materials with a perfectly plastic matrix and two-phase perfectly plastic composites—subjected to axisymmetric loading conditions. It was found that the evolution of the microstructure affects the overall response of the composite significantly. In particular, for the composite systems considered, the effective behaviour was found to exhibit hardening, or even softening, depending on the specific loading conditions, in spite of the fact that the constituents themselves were taken to be ideally plastic (i.e. non-hardening). This phenomenon is not surprising in view of the large (nonlinear) changes in the micro-geometry of the composites as they are subjected to finite deformation. More generally, these hardening–softening mechanisms would be in competition with the intrinsic hardening of the constituents of the composite (neglected in this study) and thus could have significant implications for the global stability of the material and, in particular, for the development of shear localization. We emphasize that the yield surfaces change shape and orientation as the loading progresses which cause the composite systems to develop possibly strong plastic anisotropy.

A particular focus of this part of the work was the effect of the evolution of the pair distribution function for the inclusions (voids) on the overall response of the composites. It was found that for porous composites, as well as for the more general case where the inclusions are softer than the matrix, the effect of changes in the distribution are not very significant relative to the effects of the changes in the size and shape of the inclusions (voids). In this case the simplified model of Ponte Castañeda & Zaidman (1994), which accounts only for size and shape effects, was found to be adequate. On the other hand, when the inclusions are sufficiently harder than the matrix, the deformation is concentrated in the matrix and the distribution effects tend to become very important. Thus, for example, when a composite with rigid inclusions in a perfectly plastic matrix is subjected to finite deformation, the shape and volume fraction of the inclusions do not change, but the distribution of the inclusions continues to be affected. In this case, the model of PCZ is not adequate, and it becomes essential to make use of the present (improved) model.

We also note that volume fraction of the inclusions (voids) strongly influences the magnitude of the effect of changes in the distribution – the larger the inclusion volume fraction, the stronger is the effect of changes in the distribution. However, the qualitative effects of the changes in the distribution on the overall response of the composite do not depend significantly on the inclusion volume fraction. Thus, while for very small volume fractions it may be sufficient to make use of the model of PCZ, it is essential to use the present model for larger volume fractions.

Finally, it should be mentioned that this class of models may be used to analyse the response of heterogeneous materials subjected to the complex loading conditions associated with three-dimensional forming and other manufacturing processes, provided that the scale of variation of the loading conditions is everywhere large compared to the size of the typical heterogeneity. For such non-uniform loading conditions, the microstructural variables, as well as the stress and deformation fields, would be position dependent (see, for example, the work of Wang & Richmond (1992) for hot rolling of thin plates of porous aluminium, where the porosity is found to vary both in the rolling and transverse directions). It is precisely for these situations—where direct numerical simulations, accounting for the non-uniform evolution of the microstructure, would be prohibitively expensive—that the class of simple constitutive models developed in this work, suitably modified to incorporate thermo-mechanical and other effects, could become very useful. However, before these models can be used effectively, the response of the composite to general three-dimensional loading conditions, incorporating possible changes in the orientation of the particles and of their distribution functions, must be considered. This is currently under way and the results will be reported elsewhere.

The work of M.K. and P.P.C. was supported by the NSF under Grant No. CMS-96-22714. Partial support under the MRSEC programme of the National Science Foundation Award No. DMR-96-32598 is also acknowledged. The project was begun while P.P.C. was a visiting fellow in the Department of Applied Mathematics and Theoretical Physics of Cambridge University, supported by EPSRC Grant No. GR/J66164.

References

Banks-Sills, L. & Budiansky, B. 1982 On void collapse in viscous solids. *Mech. Mater.* **1**, 209–218.

Bao, G., Hutchinson, J. W. & McMeeking, R. M. 1991 Particle reinforcement of ductile matrices against plastic flow and creep. *Acta Metall. Mater.* **39**, 1871–1882.

Budiansky, B., Hutchinson, J. W. & Slutsky, S. 1982 Void growth and collapse in viscous solids. In *Mechanics of solids, the Rodney Hill anniversary volume* (ed. H. G. Hopkins & M. J. Sewell), pp. 13–45. Oxford: Pergamon.

daSilva, M. & Ramesh, K. T. 1991 The constitutive modelling of porous metals at high rates of deformation. *J. Physique* III **1**, 909–916.

Gologanu, M., Leblond, J.-B. & Devaux, J. 1993 Approximate models for ductile metals containing nonspherical voids—case of axisymmetric prolate spheroidal cavities. *J. Mech. Phys. Solids* **41**, 1723–1754.

Gologanu, M., Leblond, J.-B. & Devaux, J. 1994*a* Approximate models for ductile metals containing nonspherical voids—case of axisymmetric oblate spheroidal cavities. *J. Engng Mater. Technol.* **116**, 290–297.

Gologanu, M., Leblond, J.-B. & Devaux, J. 1994*b* Numerical and theoretical study of coalescence of cavities in periodically voided solids. In *Computational material modeling* (ed. A. K. Noor & A. Needleman), AD-vol. 42/PVP-vol. 294, pp. 223–244. New York: ASME.

Gurson, A. L. 1977 Continuum theory of ductile rupture by void nucleation and growth. I. *J. Engng Mater. Technol.* **99**, 2–15.

Hom, C. L. & McMeeking, R. M. 1991 Plastic flow in ductile materials containing a cubic array of rigid spheres. *Int. J. Plasticity* **7**, 255–274.

Kailasam, M. & Ponte Castañeda, P. 1995 Constitutive models for porous solids in power-law creep: the effect of microstructure evolution. In *Net shape processing of powder materials* (ed. S. Krishnaswami, R. M. McMeeking & J. R. L. Trasorras), AMD-vol. 216, pp. 79–88. New York: ASME.

Kailasam, M., Ponte Castañeda, P. & Willis, J. R. 1997 The effect of particle size, shape, distribution and their evolution on the constitutive response of nonlinearly viscous composites. I. Theory. *Phil. Trans. R. Soc. Lond.* A **355**, 1835–1852. (Preceding paper.)

Koplik, J. & Needleman, A. 1988 Void growth and coalescence in porous plastic solids. *Int. J. Solids Struct.* **24**, 835–853.

Lee, B. J. & Mear, M. E. 1992 Axisymmetric deformation of power-law solids containing a dilute concentration of aligned spheroidal voids. *J. Mech. Phys. Solids* **40**, 1805–1836.

Lee, B. J. & Mear, M. E. 1994 Studies of the growth and collapse of voids in viscous solids. *J. Engng Mater. Technol.* **116**, 348–358.

McClintock, F. A. 1968 A criterion for ductile fracture by growth of holes. *J. Appl. Mech.* **35**, 363–371.

Needleman, A., Tvergaard, V. & van der Giessen, E. 1995 Evolution of void shape and size in creeping solids. *Int. J. Damage Mech.* **4**, 135–152.

Ponte Castañeda, P. 1991 The effective mechanical properties of nonlinear isotropic solids. *J. Mech. Phys. Solids* **39**, 45–71.

Ponte Castañeda, P. & Willis, J. R. 1995 The effect of spatial distribution on the effective behaviour of composite materials and cracked media. *J. Mech. Phys. Solids* **43**, 1919–1951.

Ponte Castañeda, P. & Zaidman, M. 1994 Constitutive models for porous materials with evolving microstructure. *J. Mech. Phys. Solids* **42**, 1459–1497.

Ponte Castañeda, P. & Zaidman, M. 1996 On the finite deformation of nonlinear composite materials. I. Instantaneous constitutive relations. *Int. J. Solids Struct.* **33**, 1271–1286.

Rice, J. R. & Tracey, D. M. 1969 On the ductile enlargement of voids in a triaxial field. *J. Mech. Phys. Solids* **17**, 201–217.

Wang, P. T & Richmond, O. 1992 Overview of a two state variable constitutive model for the consolidation and forming processes of powder-based porous metals. In *Mechanics of granular materials and powder systems* (ed. M. M. Mehrabadi), MD-vol. 37, pp. 63–83. New York: ASME.

Willis, J. R. 1978 Variational principles and bounds for the overall properties of composites. In *Continuum models for discrete systems* (ed. J. W. Provan), pp. 185–215. University of Waterloo Press.

Zaidman, M. & Ponte Castañeda, P. 1996 On the finite deformation of nonlinear composite materials. II. Evolution of the microstructure. *Int. J. Solids Struct.* **33**, 1287–1303.

Received 30 January 1996; accepted 10 October 1996

PHILOSOPHICAL TRANSACTIONS OF THE ROYAL SOCIETY A MATHEMATICAL, PHYSICAL & ENGINEERING SCIENCES